Heliyon

Received:
13 August 2018
Revised:
1 December 2018
Accepted:
13 March 2019

Cite as: Filomena Perri, Luca Frattaruolo, Ian Haworth, Matteo Brindisi, Asma El-magboub, Angela Ferrario, Charles Gomer, Francesca Aiello, James David Adams. Naturally occurring sesquiterpene lactones and their semi-synthetic derivatives modulate PGE2 levels by decreasing COX2 activity and expression. Heliyon 5 (2019) e01366.
doi: 10.1016/j.heliyon.2019.e01366

Naturally occurring sesquiterpene lactones and their semi-synthetic derivatives modulate PGE2 levels by decreasing COX2 activity and expression

Filomena Perri [a,1], **Luca Frattaruolo** [a,1], **Ian Haworth** [b], **Matteo Brindisi** [a], **Asma El-magboub** [b], **Angela Ferrario** [c], **Charles Gomer** [c], **Francesca Aiello** [a,*], **James David Adams** [b]

[a] *Dipartimento di Farmacia e Scienze della Salute e della Nutrizione, Edificio Polifunzionale, Università della Calabria, Arcavacata di Rende, 87036 Rende (CS), Italy*

[b] *Department of Pharmacology and Pharmaceutical Sciences, School of Pharmacy, University of Sothern California, 1985 Zonal Avenue, Los Angeles 90089, CA, USA*

[c] *Children's Hospital Los Angeles, University of Southern California, 4650 W Sunset Boulevard, Los Angeles 90027, CA, USA*

[*] Corresponding author.
E-mail address: francesca.aiello@unical.it (F. Aiello).
[1] Co-first authors equally contributed to the work.

Abstract

Plants of the Asteraceae family have been used in traditional medicine for centuries due to their main antimicrobial and analgesic activities. A liniment from *Artemisia californica* has recently been tested on patients affected by either acute pain or chronic pain conditions with great success.

The aim of this study was to evaluate the anti-inflammatory activity of sesquiterpene lactones (SLs), representing the majority in the Asteraceae family. Leucodin, α-santonin and sclareolide (three SLs) were chosen to undergo chemical modifications. This pool of molecules underwent molecular modeling

https://doi.org/10.1016/j.heliyon.2019.e01366

experiments using an in-house program, WATGEN, predicting the water network and its contribution to the overall affinity of the enzyme-ligand complex. The anti-inflammatory activity and the ability of compounds to modulate COX-2 expression have been evaluated in LPS-stimulated RAW 264.7 cells and in RIF-1 cells treated according to the Photodynamic Therapy (PDT) protocols using Photoprin (PH) as photosensitizer. Furthermore, commercially available assay kits were used to evaluate the concentration of PGE-2 and the direct inhibition of COX-2. All the tested molecules fit well in the enzyme binding pocket, but to get a substantial inhibition of the expression and activity of the enzyme as well as a reduction in the PGE2 concentration, high concentrations of the compounds are needed. The only exceptions being leucodin itself and **FP6**, one of the α-santonin derivatives, presenting a CF_3 functional group. We believe that this class of compounds has some interesting potential in the treatment of pain and inflammation. Although, the activity seems to be due to a mechanism related to the expression of the COX enzymes rather than on a direct inhibition.

Keywords: Pharmaceutical chemistry, Organic chemistry, Natural product chemistry

1. Introduction

The Asteraceae is a plentiful plant grouping, formerly known as Compositae. One of the largest genus is the *Artemisia* one with over 500 species. It is believed that the genus is named after Artemis, the Greek goddess of hunt, forests and childbirth, who gave artemisian plants to Chiron the Centaur (Wright, 2002). Common names, instead, include mugwort, wormwood and sagebrush. It is characterized by a great phytochemical variability according to the different geographical origins. In fact, they often are aromatic perennial herbs or low shrubs common in northern temperate areas in Asia, Europe, North America and North Africa (Good, 1974). Some general features are alternate leaves, tiny flower heads, a flat, naked receptacle and tubular florets (Allaby, 2006). Some species are grown with ornamental purposes and others, with the peculiar bitter taste of their leaves, are used as culinary herbs (*A. dracunculus*, for instance); although, medicinal properties are the ones worth considering. The importance of the *Artemisia* genus has been frequently highlighted in folk-medicine, in fact these plants were used throughout different cultures such as European, Chinese, Mexican, Chumash Indian, etc.

The most well-known *Artemisia* plant is certainly *A. Annua*, for its anti-malarian activity. In ancient Chinese texts, it is called either *cao hao* or *qing hao*. As far back as 168 BC, it was recommended for the treatment of haemorrhoids, later also for intermittent fevers, lingering pain in bones and joints, etc. Nowadays, in the current Chinese pharmacopeia, the infusion of the dried herb is listed for the treatment of fevers and malaria

https://doi.org/10.1016/j.heliyon.2019.e01366

(Willcox, 2009). This potent antimalarial activity is due to a sesquiterpene lactone, named artemisinin and derivatives of this molecule are now established as antimalarial drugs (Klayman, 1993). Chumash Indians adopted several Asteraceae members for their pain-relieving activity. *A. californica*, also known as California Sagebrush, was an important remedy as well: a poultice or hair wash for headache (Timbrook, 1990), a decoction of the leaves and stems externally for colds, asthma and arthritis (Adams, 2012) and a liniment made from this plant, bear grease or whale oil was used as a topical pain-killer. Recently, a new alcoholic liniment based on the original recipe with some variations, has showed interesting results in pain patients affected by arthritis, muscle and ligament strains, bruises, broken bones, low back pain and cancer (Adams, 2012). *A. californica*, was used also by Costanoan Indians for toothache and to poultice wounds (Adams, 2012). Finally, it is worth noticing its capability, maybe due to the presence of flavonoids, of inhibiting NO production, opening the possibility of future anti-inflammatory uses (Messaudene, 2011). These activities are due to the varied and numerous classes of compounds present in the genus. They include: terpenoids, alkaloids, phenolics and polyacetylenes. One of the most prevalent and biologically relevant groups of molecules are sesquiterpenoids. They can account for a great proportion in the Asteraceae family and especially in the *Artemisia* genus.

Particularly, sesquiterpenoids that possess a lactone ring, precisely called sesquiterpene lactones (SLs), have raised attention in the medicinal chemistry field, due to their numerous biological activities, also known before the so-called "modern medicine". Studies on SLs benefits in people focus on their anti-cancer activity; their potential is so impressive that some compounds entered clinical trials (Ghantous et al., 2010). Their use as antimalarials has been known for centuries and they have emerging roles in the treatment of cardiovascular diseases and other disorders such as diarrhoea, flu, and burns. Plus, they are responsible for other effects in the prevention of neurodegeneration (Rodriguez et al., 1976). SLs are also alleged to reduce stomach ulcers protecting the gastric lining (Giordano et al., 1990). Not to mention their well-known anti-inflammatory and analgesic properties, afterwards discussed in detail (see Fig. 1).

Leucodin, also called leukomisin and desacetoxymatricarin, isolated from several plants in the genus *Artemisia* including *Artemisia californica* (Adams, 2012;

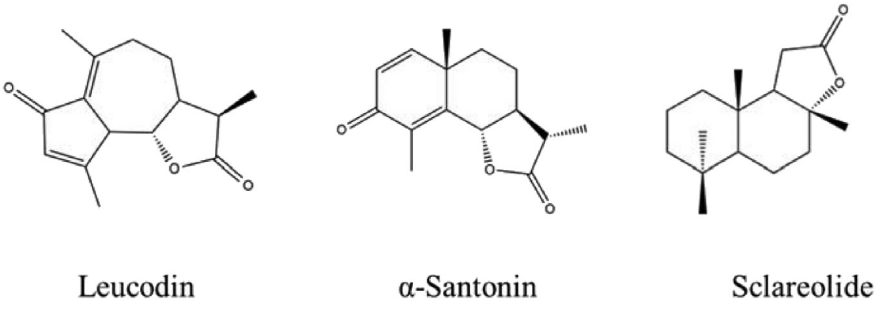

Fig. 1. Leucodin, α-santonin and sclareolide structures.

https://doi.org/10.1016/j.heliyon.2019.e01366

Fontaine et al., 2013) is part of the pseudoguaianolides group. It is characterized by a cyclopentadienone rigid ring system. In leucodin, the lactone is in a 6α,7β conformation. The cyclopentadienone and perhaps the lactone rings may react with thiols in proteins to provide biological activity. Leucodin has been reported to inhibit COX2 (IC_{50} 129 μg/ml) and inducible nitric oxide synthase, IC_{50} 160 μg/ml (Schmidt et al., 2008). Furthermore, guaianolides have often been highlighted for their potential use in several conditions (Simonsen et al., 2013). It seemed, therefore, interesting to choose leucodin within the SLs present in *A. californica* to further study molecules with this carbon backbone. Unfortunately, most of the time sesquiterpenoids cannot be synthesised cost-effectively and extraction requires a lot of time and funds, too. Due to its cost, in fact, leucodin was purchased in such a small amount that attempts in synthesising derivatives were not advisable. Aiming to have a little variety in the carbon backbone, an eudesmanolide was taken into consideration: α-santonin. α-Santonin has been extracted from several *Artemisia* species, formerly used as an anthelminthic, but then removed from the market due to its serious hazards to patients' health. King's American Dispensatory of 1898 noted that oral administration of α-santonin could produce convulsions and death from respiratory paralysis as well as xanthopsia.

Nowadays it is a promising agent for the synthesis of derivatives with anti-inflammatory and cytotoxic activity. It showed, in fact, strong anti-inflammatory, antipyretic and analgesic properties against carrageenan-induced edema in rat paw. The exact mode of action is not elucidated, but it may be due to the suppression of kinin and prostaglandin formation (Al-Harbi et al., 1994).

A derivative of santonin, (11S)-2α-bromo-3-oxoeudesmano-12,6α-lactone, was found to inhibit NF-kB translocation into the nucleus (Tamura et al., 2012). Santonin analogues have been synthesized and tested as cytotoxic agents for anticancer activity (Arantes et al., 2010; Ferreira et al., 2013). Inhibition of 5-lipoxygenase has been reported for some santonin derivatives (Schwarz et al., 2007). Santonin and its analogues also inhibit macrophage nitric oxide synthase (Chen et al., 2014), which is involved in inflammation. Moreover, a synthesis of leucodin from santonin has been reported (White et al., 1969), thus it seemed a great shortcut to get the so precious pseudoguaianolide. Unfortunately, this synthesis pathway is not only long and intricate, but also it involves a photochemical approach, which turned out to be not available nor possible at that moment. Nevertheless, α-santonin was chosen for its structural peculiarities and known biological properties; besides, being commercially available at an affordable price, it allowed the synthesis of several derivatives. Finally, to assess whether the lactone itself has a role, a molecule with no other functional moieties needed to be tested. Sclareolide was then picked. Sclareolide, also called norambreinolide, is a fragrance used in cosmetics. It has been isolated from various species of *Salvia* and several other plants. It has the same labdane structure as the related compound sclareol. Concerning inflammation,

https://doi.org/10.1016/j.heliyon.2019.e01366

sclareol was shown to decrease nitric oxide (NO) production, and the expression of the inducible nitric oxide synthase (iNOS) and cyclooxygenase-2 (COX-2) proteins (Huang et al., 2012; Zhong et al., 2012; Coricello et al., 2018; Carullo et al. 2016). Both sclareol and sclareolide demonstrated good antibacterial activities (Hayet et al., 2007). In addition to that, a German patent studied diterpenes with a labdane structure (i.e. sclareol, sclareolide, ambrox, ambroxdiol) suitable for anti-inflammatory use (Gerke et al., 2001). Sclareolide inhibited 5-lipoxygenase with an IC_{50} of 1 mg/ml. The aim of this study was to produce α-santonin and sclareolide derivatives and to evaluate their anti-inflammatory activity in order to study the structure-activity relationship of the new sesquiterpenic analogues.

2. Methods and materials

2.1. Organic synthesis

All reagents were purchased from Sigma Aldrich. All the reactions were monitored by TLC on 0.2 mm silica gel 60 F254 plates (Merck) using 254 and 365 nm UV light or a solution of H_2SO_4 and consequent heating to detect the spots. To purify the obtained compounds chromatographic columns were run using silica gel Merck 60, 230−400 mesh, 0.040−0.063 mm as a stationary phase. Melting points were recorded on a Gallenkamp 21374 melting point apparatus. Mass spectra were recorded on an Agilent Technologies 6200 series LCMS instrument (property of USC School of Pharmacy). HRMS were measured on an Agilent Technologies 1200 series LCMS instrument (property of California Institute of Technology). ^{1}H and ^{13}C NMR spectra were acquired on Varian 400 MHz instruments (property of University of Southern California) by applying pulse sequences which are commonly used for the structural analysis of synthetic natural compound analogs (Di Gioia et al., 2017). $CDCl_3$ and TMS were used as the solvent and spectral calibrating agent, respectively. Organic phases were concentrated under reduced pressure and dried on anhydrous Na_2SO_4.

Since the lactone in this study is alleged to be mainly responsible for the activity, there was no intention on modifying it. Therefore, concerning α-santonin, the ketone was the target as shown in Fig. 2.

The main purpose was to convert α-santonin into its oxime (**FP1**) and perform reactions that would have led to the so-called oxime ethers. These compounds have recently drawn much attention in medicinal chemistry on account of their significant bioactivity and their importance in medicine, agriculture and organic synthesis is well known in literature (Abid et al., 2005). To the best of our knowledge, only two examples of *O*-alkylated oxime derivatives for α-santonin have been reported: α-santonin methoxime (Kang et al., 2014), which was also obtained in this experiment (**FP6**) and α-santonin allyloxyme (Merkhatuly et al., 2007). The choice of the substituents was made to have the highest possible chemical variability, since a similar study does still not exist.

https://doi.org/10.1016/j.heliyon.2019.e01366

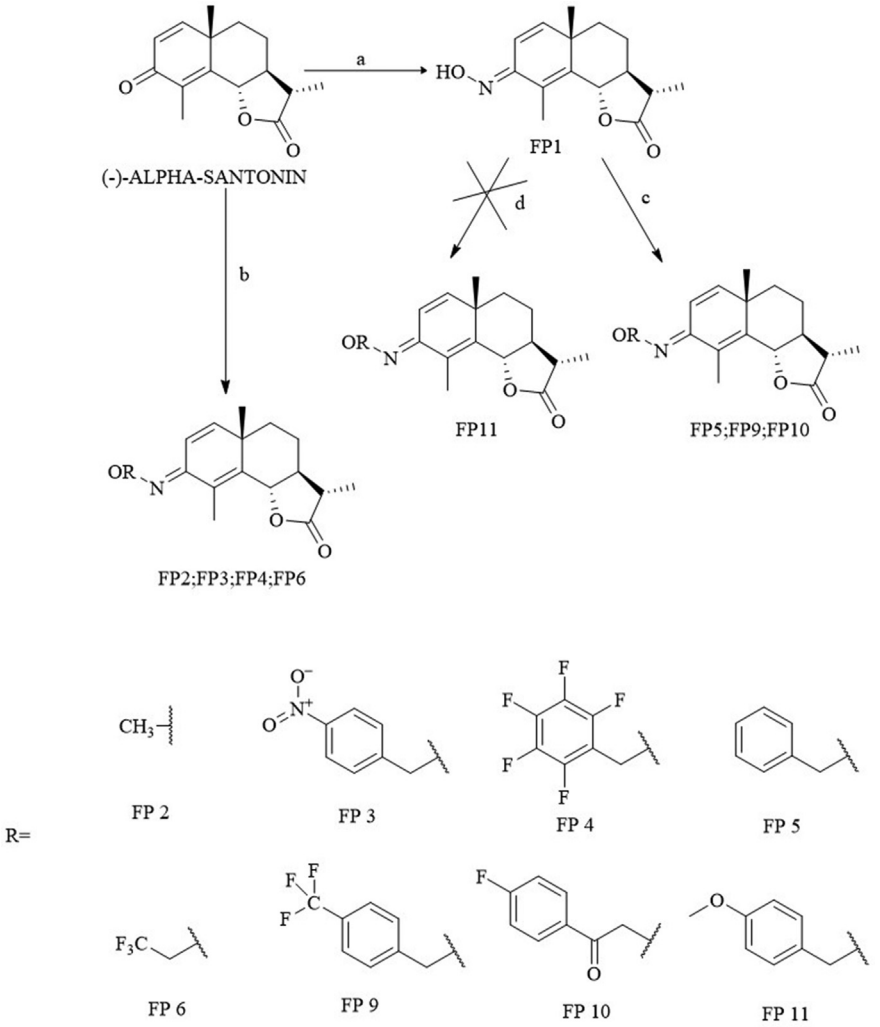

Fig. 2. Reagents and conditions: a $NH_2OH{\cdot}HCl$, Py, 115 °C; b NH_2OR HCl, Py, 115 °C; c R-CH_2-Br, Potassium tert-butoxide, DMF, 80−90°; d C R-OH, PPh_3, NBS, DBU, TBAB, Anhyd MeCN, 80 °C.

From the literature, three main ways to obtain oxime ethers resulted:

- Using an already *O*-alkylated hydroxylamine hydrochloride and making it react with alpha-santonin itself (b) (Kang et al., 2014);
- Starting from the santoninoxime, making it react with an alkyl bromide (c) (Merkhatuly et al., 2007);
- A one-pot procedure involving the oxime and an alcohol (d) (Soltani Rad et al., 2010)

Method (b) was very effective and basically follows the same mechanism as the formation of the oxime with the difference that the hydroxylamine already has the substituent on the oxygen. The lowest yield (11%) was achieved for FP3. The reason could be the presence of the nitro group which is a very strong electron-

https://doi.org/10.1016/j.heliyon.2019.e01366

withdrawing group and removes electron density from the system. Substituents containing fluorine atoms also did not get to high yields (38.2% for FP4 and 25% for FP6), but still higher than FP3. This is very likely because with halogens, inductive and resonance properties are competing and, even though the induction is prevailing, the general withdrawing effect is less powerful than the one produced by the $-NO_2$. After all, this procedure is straightforward and worked well.

Method (c) was very effective with alkyl bromides easily leading to FP5 and FP9.

Method (d) to get to **FP11** was not successful. This is most likely due to two main changes in the procedure described by the reference: N-bromosuccinimide (NBS) instead of CCl_4 and tetrabutylammonium bromide (TBAB) instead of tetrabutylammonium iodide (TBAI). NBS was used because of the well-known CCl_4 carcinogenicity and TBAB was used because it was the one immediately available in our laboratories. The authors themselves say that using another phase-transfer catalyst instead of TBAI was not effective and using other reagents as sources for positive-halogen such as NBS did not afford satisfactory results. This alkylation, however, was very interesting because of the high availability of different alcohols, so it was worth a try, but no other similar reactions were performed.

Derivatives of the non-aromatic sesquiterpene lactone sclareolide were synthesized, too (Fig. 3). Since the lactone is the only functional group in the molecule, reactions aiming at that area could be useful to attest to the relevance of the lactone in the biological activity and how, the further chemical modifications could influence it.

Focusing on the lactone moiety, its reduction to a diol (**FP7**) was performed using lithium aluminium hydride (Zoretic and Fang, 1998).

No other modifications were made on the two free hydroxyl groups because it was firstly important to see if opening the lactone was deleterious for the eventual activity.

The last modification was designed to evaluate if a thionolactone could be more effective than the lactone, for example, regarding the nature of the hydrogen bond formation. It is known, in fact, that hydrogen bonds to sulfur in a quite different way than oxygen in terms of strength and geometry of the bond (Platts et al., 1996; Wierzejewska and Saldyka, 2004).

Lawesson's reagent is a very effective mild thionating agent which easily led to the wanted result (FP8).

2.2. Docking studies

The COX-2 structure was obtained as a 4PH9 crystal from the Protein Data Bank. This crystal is for Ibuprofen bound to COX-2. The protein was cleaned up and

https://doi.org/10.1016/j.heliyon.2019.e01366

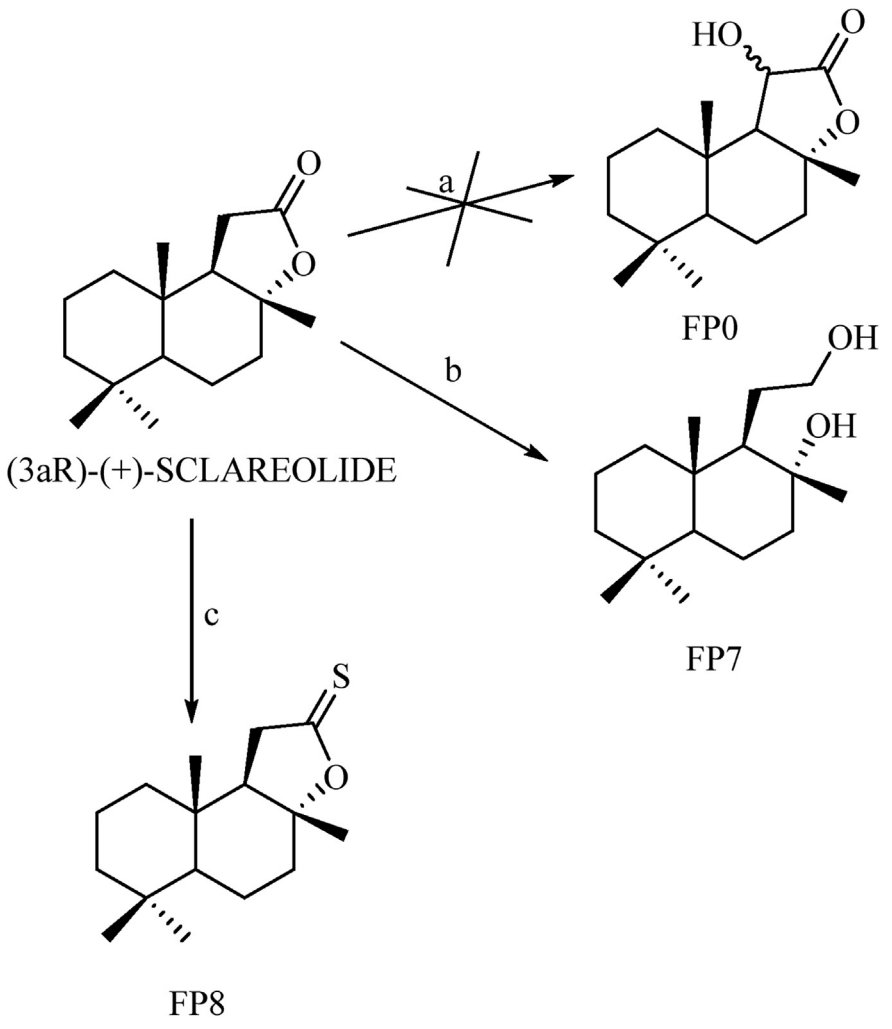

Fig. 3. Reagents and conditions: a see text; b LAH, anhydrous THF, 66 °C; c Lawesson's Reagent, anhydrous. Toluene, 110−115 °C.

uploaded to Autodock Vina. A Vina search box was defined to include the COX channel (Arg 120, Tyr 355 and Tyr 385). In order to validate the approach, ibuprofen was docked first and the resultant models compared to the crystal structure. Ibuprofen docking model 2 was quite similar to the crystal structure (data not shown). All the molecules were docked using the same approach. Each docking process resulted in 9 models; all the 9 models were checked and all off-target models were excluded. The accepted models were then subjected to solvation using WATGEN (Bui et al., 2007). Solvated complexes were studied in three ways:

a) the water network was analyzed and water molecules were classified as reported by Li et al., 2011

b) energetically water molecules were classified to be stabilized, destabilized and unchanged, in addition displaced water molecules were counted.

https://doi.org/10.1016/j.heliyon.2019.e01366

Note: a) and b) were done using in-house codes.

c) the interactions were further visualized using LigPlot (http://www.ebi.ac.uk/thornton-srv/software/LIGPLOT/).

2.3. Biological assays

2.3.1. Cell cultures

Murine macrophages RAW 264.7 cell line has been purchased from the American Culture Collection (ATCC, Manassas, VA) and cultured in DMEM (Sigma) supplemented with 10% fetal bovine serum (FBS, Sigma), 2 mM L-glutamine (Gibco, Life Technologies) and 1% penicillin/streptomycin (Gibco, Life Technologies). Mouse RIF-1 (Radiation induced Fiber sarcoma) cells were grown in RPMI 1640 supplemented with 15% fetal calf serum (FCS) antibiotics (100 units Pen and 100 units Strep/ml) and L-glutamine (to 1 nM). Cells were cultured at 37 °C in 5% CO2 in a humidified atmosphere.

2.3.2. Immuno-enzymatic quantification of prostaglandin E2 in human blood

To evaluate changes in PGE2 release, an immuno-enzymatic assay (Invitrogen, Thermofisher) has been used as previously reported (Siracusa et al., 2011). Briefly, 1 mL of heparinized peripheral blood aliquots, from healthy volunteers, has been incubated with different concentrations of compounds for 24 h at 37 °C, both in the absence and in the presence of 10 μg/mL LPS. Then the contribution of platelet COX-1 was suppressed by adding aspirin (10 μg/mL) at time 0. Next, plasma was separated by centrifugation and used for ELISA tests, following manufacturer indications. NS-398 (5 μM), a selective COX-2 inhibitor has been used as a positive control.

2.3.3. COX-2 expression immunoblot analysis in RAW 264.7 cells

RAW 264.7 cells were grown to 70−80% confluence, treated with 100 μM FP6 for 24 hours, and lysed as previously described. Briefly, cells were lysed in 200 μL of 50 mM Tris−HCl, 150 mM NaCl, 1% NP-40, 0.5% sodium deoxycholate, 2 mM sodium fluoride, 2 mM EDTA, 0.1% SDS, containing a mixture of protease inhibitors (aprotinin, phenylmethylsulfonyl fluoride, and sodium orthovanadate; Sigma Aldrich) for total protein extraction. The same amounts of proteins were resolved on 15% SDS-polyacrylamide gel, transferred to a nitrocellulose membrane and probed with a COX-2 specific antibody (Santa Cruz, Biotechnology, CA, USA) (Bonesi et al., 2018). To confirm equal loading and transfer, membranes were stripped and incubated with anti-GAPDH antibody (Santa Cruz, Biotechnology, CA, USA).

https://doi.org/10.1016/j.heliyon.2019.e01366

The antigen-antibody complex was detected by incubation of the membranes with peroxidase-coupled goat anti-mouse or goat anti-rabbit antibodies and revealed using the ECL System (Amersham Life Science, Chicago, IL) (Lee et al., 2014).

2.3.4. Inhibition of NO production in LPS-stimulated RAW 264.7 cells

The presence of nitrite, a stable oxidized product of NO, was determined in cell culture media by the Griess reagent [1% sulfanamide and 0.1% N-(1-naphthyl)ethylenediamine dihydrochloride in 2.5% H3PO4] (Tundis et al., 2018). RAW 264.7 cells were seeded in 24-well plates with a density of 2×10^5 cells/well and cultured in complete medium overnight. Cells were then treated, simultaneously, with LPS (1 μg/mL) and different concentrations of compounds for 24 h. DMSO (Sigma Aldrich) was used as a vehicle control. After treatment end, 100 μL of cell culture supernatant was combined with 100 μL of Griess reagent in a 96-well plate followed by spectrophotometric measurement at 550 nm using a microplate reader.

2.3.5. Cell viability assay in RAW 264.7 cells

Cell viability was determined by using 3-(4,5-Dimethyl-2-thiazolyl)-2,5-diphenyl-2H-tetrazolium bromide (MTT, Sigma) assay as described previously (Frattaruolo et al., 2017). Briefly, cells have been treated with different concentrations of compounds for 24 hours and, after treatment, MTT solution was added to each well (to a final concentration of 0.5 mg/mL) and plates were incubated at 37 °C for 2 h until the formation of formazan crystals. DMSO-solubilized formazan in each well was quantified by absorbance at 570 nm using a microplate reader.

2.3.6. Immuno-enzymatic quantification of prostaglandin E2 in LPS-stimulated RAW 264.7 cells

To quantify PGE2 production in LPS-stimulated RAW 264.7, cells were treated as mentioned for cell viability assay, in presence of absence of LPS, and, after 24 h, the medium of treated cells was collected and subjected to immuno-enzymatic assay (Invitrogen, Thermofisher), following manufacturer indications.

2.3.7. Photodynamic therapy (PDT) protocols in RIF-1 cells

RIF-1 cells were trypsinized, counted using a hemocytometer and seeded (1.5×10^6 cells per dish for protein and PGE2 analysis, 150 cells per dish for clonogenic assay control and alpha Santonin alone and 450 cells per dish for clonogenic assay of cells receiving Photofrin mediated PDT ± alpha Santonin) in 60 mm plastic Tissue culture dishes and incubated overnight in complete growth media. Cells were then incubated in the dark with PH (25 ug/ml) for 16 h at 37 °C in RPMI 1640 media

https://doi.org/10.1016/j.heliyon.2019.e01366

supplemented with 5% FCS, then washed for 30 min in fresh growth media, rinsed with unsupplemented RPMI and exposed to 900 mJ/cm2 red light at 630 nM generated using a Diode laser (DioMed 630 PDT). Treated cells were refed with 3 ml complete growth media (+/- alpha Santonin and/or DMSO/Ethanol) to determine clonogenic survival or 1.5 ml serum-free media (+/- alpha Santonin and/or DMSO/Ethanol) for analysis of COX-2 expression and PGE2 secretion. Cells were incubated with α-santonin or DMSO immediately after light treatment at concentrations indicated in each experiment. Cells used for clonogenic assay were allowed to grow for 7 days, then fixed with 70% ethanol and stained using methylene blue. Colonies were counted and % Survival determined via comparison with the number of colonies that formed in dishes of control cells (Received no PDT or α-santonin). Cells and media used for COX-2 expression and secreted PGE2 levels were harvested 24 hours after treatment.

2.3.8. WST-1 assay

RIF-1 cells were seeded in 96 well plates ($7-10 \times 10^3$/100 ul/well) to measure viability and treated as described in "In vitro treatment protocol". Cell viability was evaluated at 24 h after treatment using a WST-1 (2-(4-iodophenyl)-3-(4-disulfophenyl)-2H-tetrazolium, monosodium salt) cell proliferation assay (Roche Applied Science, Indianapolis, IN) as per manufacturer's instruction. Plates were read using a MR600 microplate reader (Dynatech, Golden Valley, MN) at 450 nm.

2.3.9. COX-2 expression immunoblot analysis in RIF-1 cells

COX-2 expression was documented by Western immunoblot analysis. Twenty-four h after PDT, RIF-1 cells were scraped off the culture dishes with rubber policemen and transferred to new 15 ml conical tubes. Tubes were spun at 1000 rpm for 5 minutes, the supernatants collected and stored at − 20 °C for PGE2 analysis. The pellets were sonicated in 120 μl of 1X cell lysis buffer (Cell Signaling Technology, Danvers, MA) containing 1 μM phenylmethylsulfonyl fluoride (Sigma, St. Louis, MO), spun at 15,000 rpm and supernatants stored at -20 C for Western immunoblot analysis. Protein concentration of each sample was determined by Bio Rad Protein Assay (Life Science Research, Hercules, CA). Eighty μg protein samples were size-separated on discontinuous gradient polyacrylamide gels (8−16%) and transferred to nitrocellulose membranes. Membranes were blocked for 1 h with 5% nonfat dry milk and then incubated overnight with a mouse monoclonal anti-COX-2 (BD Transduction Laboratories, San Diego, CA). Membranes were then incubated with an anti-mouse peroxidase conjugate (Sigma) and the resulting complexes were visualized by enhanced chemiluminescence autoradiography (Amersham Life Science, Chicago, IL) to document COX-2 expression in RIF-1 cells. Protein loading was evaluated by incubating the same filters with a mouse monoclonal anti-actin antibody

https://doi.org/10.1016/j.heliyon.2019.e01366

(MP Biochemicals, Aurora, OH). Autoradiographs were quantified by scanning densitometry.

2.3.10. Immuno-enzymatic quantification of prostaglandin E2 in RIF-1 cells

A PGE2 enzyme immunoassay kit (Cayman Chemical Co, Ann Arbor, MI) was used according to the manufacturer's instructions to quantify PGE2 concentrations in RIF-1 cells culture media. The 96 wells plate of the kit is coated with Goat Polyclonal Anti-Mouse IgG. This Competitive Enzyme Immunoassay is based on the competition between PGE2 present in the culture media and a PGE2-acetylcholinesterase conjugate called Tracer (provided by the kit) for a limited amount of PGE2 mouse monoclonal antibody (provided by the kit) in the well. The amount of the Tracer that is able to bind to the PGE2 monoclonal antibody and immobilized by the binding with the coated Anti-mouse IgG will be inversely proportional to the concentration of PGE2 of the culture media loaded in the well. The plate is washed to remove any unbound reagents and the Acetylcholinesterase substrate is added to each well. The product of this enzymatic reaction has a yellow color and absorbs at 410 nm. The intensity of this color, determined spectrophotometrically, is inversely proportional to the amount of PGE2 present in the culture media of each well.

The kit provides PGE2 of known concentration to prepare a standard curve (correlating 410 nm OD readings with PGE2 concentrations) used to calculate the unknown PGE2 levels in RIF-1 cells culture media.

2.3.11. COX-2 inhibition assay

The inhibitory activity of the synthesized compounds against COX-2 was determined exploiting the commercially available COX Inhibitor Screening Assay (Cayman Chemical, Ann Arbor, MI, USA, catalogue no. 560131), which uses an enzyme immunoassay to measure PGE2a produced by stannous chloride reduction of PGEH2, derived in turn by reaction between the target enzyme and the substrate, arachidonic acid. According to manufacturer's protocol, test compounds (10 μL) were incubated for 10 min at 37 °C with assay buffer (0.1 M Tris-HCl, pH 8, 160 μL), Heme (10 μL), and human recombinant COX-2 enzyme solution (10 μM). Arachidonic acid (10 μL) was then added, and the resulting mixture was incubated for 2 min at 37 °C. Enzyme catalysis was stopped by adding HCl (1M, 10 mL) and the obtained PGEH2 was converted to PGE2a with saturated stannous chloride solution (20 mL). Prostanoids were finally quantified by EIA and their amount was determined through interpolation from a standard curve. The % inhibition of target enzyme by test compounds was calculated by comparing PGE2a produced in compound-treated samples with that of compound-free, control sample. The highly

https://doi.org/10.1016/j.heliyon.2019.e01366

potent COX-2 inhibitor Dup-697 was used as the reference compound. All the test derivatives were dissolved into dilute assay buffer and their solubility was facilitated by using DMSO, whose concentration never exceeded 1% in the final reaction mixture. The inhibitory effect of the compounds was routinely estimated at a concentration of 10 μM.

2.3.12. Statistical analysis

Data are presented as mean values ± standard deviation, taken over ≥3 independent experiments, with ≥3 replicates per experiment, unless otherwise stated. Statistical significance was measured by using one-way analysis of variance (ANOVA) test. P value ≤ 0.05 was considered statistical significant. Non-linear regression analysis (GraphPad Prism 7) was used to generate sigmoidal dose-response curves to calculate IC50 values.

3. Results and discussion

3.1. Synthesis

- (-) - α -Santoninoxime (FP1) The procedure described by the reference (Merkhatuly et al., 2007) was followed (0.4 g, 77%). Mp: 216 °C, Molecular Formula: C15H19NO3, MW: 261,32 g/mol., 1H-NMR (400 MHz, CDCl3), δ, ppm: 6.9 d, 6.02 d, 4.8 dd, 2.39 dq, 2.13 s, 2.0−1,96 m, 1.84−1.58 m, 1.50 dt, 1.26 s, 1.25 d., 13C-NMR (100 MHz, CDCl3), δ, ppm: 178.06, 151.26, 145.39, 138.95, 122.70, 122.19, 82.22, 53.45, 41.03, 40.84, 38.26, 25.83, 23.75, 12.44, 12.07, 1.90., MS (ESI,70 eV): *m/z (%)* = 262.01 [M + H+] (100).
- (-) - α -*Santonin methyloxime* (FP2) The same procedure seen for FP1 was followed (0.25 g, 45%). Mp: 176.2 °C Molecular Formula: C16H21NO3, MW: 275,34 g/mol, 1H-NMR (400 MHz, CDCl3), δ, ppm: 6.81 (d, J = 10.1 Hz, 1H), 5.97 (d, J = 10.1 Hz, 1H), 4.78 (dd, J = 11.1, 1.3 Hz, 1H), 3.93 (s, 3H), 2.34 (dq, J = 12.1, 6.9 Hz, 1H), 2.15 (s, 3H), 2.02−1.94 (m, 1H), 1.84−1.58 (m, 3H), 1.48 (td, J = 12.8, 4.4 Hz, 1H), 1.25 (d, J = 6.9 Hz, 3H), 1.24 (s, 3H), 13C-NMR (100 MHz, CDCl3), δ, ppm:178.1, 149.87, 145.09, 138.28, 122.85, 112.85, 82.31, 61.98, 53.43, 41.04, 40.7, 38.28, 25.82, 23.77, 12.43, 11.99,MS (ESI,70 eV):*m/z (%)* = 276.02 [M + H+] (100).
- (-) - α -*Santonin (4-nitro)benzyloxime ether* (FP3) The same procedure seen for FP1 was followed, the reagents being 0.493 g of (-)-α- santonin (2.0 mmol) and 0.49 g of O-(nitrobenzyl)hydroxylamine hydrochloride (2.4 mmol) in 3 mL of pyridine. Regarding the purification, a column chromatography was run using

https://doi.org/10.1016/j.heliyon.2019.e01366

ethyl acetate 17% in hexane as the eluent. The product was recrystallized from ethanol, giving white aciform crystals (92.2 mg, 11%). Mp: 145.5 °C. Molecular Formula: C22 H24 N2 O5 MW: 396,44 g/mol. 1H-NMR (400 MHz, CDCl3), δ, ppm: 8.21 (d, J = 8.8 Hz, 2H), 7.53 (d, J = 8.8 Hz, 2H), 6.88 (d, J = 10.4 Hz, 1H), 6.03 (d, J = 10.4 Hz, 1H), 5.25 (s, 2H), 4.78 (dd, J = 11.2 Hz, 1.6 Hz, 1H), 2.34 (dq, J = 12.1 Hz, 6.9 Hz, 1H), 2.10 (s, 3H), 2.0−1.96 (m, 1H), 1.83−1.60 (m, 3H), 1.51 (td, J = 12.8 Hz, 4.4 Hz, 1H), 1.26 (s, 3H),1.24 (d, J = 6.9 Hz, 3H) . 13C-NMR (100 MHz, CDCl3), δ, ppm: in progress. HRMS (ESI, 70 eV): *m/z* (%): calculated = 397.165, found = 397.177

- (-) - α -*Santonin (2,3,4,5,6-pentafluoro)benzyloxime ether (*FP4). The same procedure seen for FP1 was followed, the reagents being 0.2 g of (-)-α-santonin (0.83 mmol) and 0.250 g of O-(2,3,4,5,6-pentafluorobenzyl)hydroxylamine hydrochloride (1 mmol) in 3 mL of pyridine. Concerning the purification a column chromatography was run using EtOAc 20% → 100% in hexane as the eluent. The product is a yellow oil (0.14 g, 38.2%). Molecular formula: C22H20 F5 NO3, MW: 441,14 g/mol, 1H-NMR (400 MHz, CDCl3), δ, ppm: 6.74 (d, J = 10.4 Hz, 1H),5.98 (d, J = 10.0 Hz, 1H), 5.21 (s, 2H), 4.75 (dd, J = 11.2 Hz, 1.2 Hz, 1H), 2.33 (dq, J = 12.1 Hz, 6.9 Hz, 1H), 2.09 (s, 3H), 1.99−1.94 (m, 1H), 1.80−1.58 (m, 3H), 1.45 (td, J = 12.8 Hz, 4.4 Hz, 1H) 1.26 (s, 3H), 1.24 (d, J = 6.9 Hz, 3H), 13C-NMR (100 MHz, CDCl3), δ, ppm: 11.79, 12.42,23.68, 25.69, 30.50, 38.20, 40.76, 40.99, 53.44, 62.53, 82.19, 112.64, 122.67, 139.23, 145.82, 150.89, 177.98, 19F-NMR, δ, ppm: -141.99 (d, J = 13.70, 2 F: 1,5), -153.95 (s, 1 F: 3), -162.51 (t, J = 10.35, 2 F: 4, 6), HRMS (ESI,70 eV):*m/z (%):* calculated = 442.1436, found = 442.1447.
- (-) - α -*Santonin Benzyloxime ether (FP5).* A 25 mL round-bottomed flask was fitted with a reflux condenser and a Teflon-covered stirring bar. The flask was firstly charged with 0.3 g of santoninoxime (1.14 mmol) and 0.135 g of potassium *tert*-butoxide (1.14 mmol) in 6 mL of DMF. Under stirring, 0.15 mL of benzyl bromide (1.14 mmol) was then added. The mixture was heated at 80−90 °C and it was monitored via TLC, using Petroleum Ether: Ethyl acetate 2:1 as the eluent. After 20 hours, no further improvement was detected and the reaction was quenched, the solvent removed under reduced pressure and the residue washed with water three times. The organic phase was dried over Na2SO4, filtered and concentrated. Purification was achieved with column chromatography using EtOAc 15% → 100% in Petroleum Ether as the eluent. The product is a white crystal (0,055 g, 14%). Mp: 148 °C, Molecular Formula: C22 H24 NO3, MW: 351.43 g/mol, 1H-NMR (400 MHz, CDCl3), δ, ppm: 7.38−7.26 (m, 5H), 6.87 (d, J = 10.4 Hz, 1H), 5.95 (d, J = 10.4 Hz, 1H), 5.17 (s, 2H), 4.77 (dd, J = 11.2 Hz, 1.6 Hz, 1H), 2.34 (dq, J = 12.1 Hz, 6.9

https://doi.org/10.1016/j.heliyon.2019.e01366

Hz, 1H), 2.15 (s, 3H), 2.0−1.96 (m, 1H), 1.83−1.60 (m, 3H), 1.48 (td, J = 12.8 Hz, 4.4 Hz, 1H), 1.26 (s, 3H),1.23 (d, J = 6.9 Hz, 3H), 13C-NMR (100 MHz, CDCl3), δ, ppm: 12.04, 12.43, 12.67, 23.71, 25.79, 38.25, 40.70, 40.98, 53.43, 77.09, 82.28, 113.11, 122.87, 127.72, 128.28, 128.30, 137.97, 138.47, 145.11, 150.10, 175.86, 178.18, MS (ESI,70 eV): 351 [M] (100).

- (-) - α -*Santonin (2,2,2-trifluoroethyl)oxime ether* (FP6). The same procedure seen for FP2 was followed, the reagents being 0.338 g of (-)-α- santonin (1.37 mmol) and 0.259 g of 2,2,2-Trifluoroethoxyamine hydrochloride (1.65 mmol) in 3 mL of pyridine. Purification by column chromatography with EtOAc 25% → 100% in hexane led to the product as beige crystals (0.13 g, 25%). Mp: 75.5 °C, Molecular formula: C17H20F3NO3, MW: 344,81 g/mol, 1H-NMR (400 MHz, CDCl3), δ, ppm: 6.84 (d, J = 10.4 Hz, 1H), 6.05 (d, J = 10.4 Hz, 1H), 4.78 (dd, J = 11.2 Hz, 1H), 4.49 (s, 2H) 2.34 (dq, J = 12.1 Hz, 6.9 Hz, 1H), 2.13 (s, 3H), 2.0−1.96 (m, 1H), 1.83−1.60 (m, 3H), 1.51 (td, J = 12.8 Hz, 4.4 Hz, 1H), 1.26 (d, J = 6.9 Hz, 3H) 1.25 (s, 3H) ppm, 13C-NMR (100 MHz, CDCl3), δ, ppm: 12.0, 12.54, 23.66, 25.84, 29.72, 38.16, 41.18, 53.63, 70.98, 82.27, 112.94, 122.54, 140.05, 146.46, 151.84, 178.28, 19F-NMR, δ, ppm: -73.846 (CF3), HRMS (ESI,70 eV): calculated = 344.1468, found 344.1475.
- (-) - α -*Santonin (4-trifluoromethyl)benzyloxime ether* (FP9). A 10 mL round-bottomed flask was fitted with a reflux condenser and a Teflon-covered stirring bar. The flask was first charged with 0.1 g of santoninoxime (0.38 mmol) and 0.042 g of potassium *tert*-butoxide (0.38 mmol) in 2 mL of DMF. Under stirring, 0.09 g of (4- trifluoromethyl)benzyl bromide (0.38 mmol) was then added. The mixture was heated at 80−90 °C and it was monitored via TLC, using Hexane: Ethylacetate 1:1 as the eluent. After 20 h, there was still some starting material, but no more bromide. So, additional 0.045 g of (4- trifluoromethyl)benzyl bromide and 0.021 g of potassium *tert*-butoxide were added. After 2 more hours, the reaction was quenched. Work-up was the same as seen for FP5. Purification was achieved with column chromatography using EtOAc 10% in hexane as the eluent. The product was a colourless oil (0.025 g, 16%). Molecular Formula: C23 H24 F3 NO3, MW: 419,17 g/mol, 1H-NMR (400 MHz, CDCl3), δ, ppm: 7.59 (d, J = 8.1 Hz, 2H, Ar-H), 7.52 (d, J = 8.1 Hz, 2H, Ar- H), 6.87 (d, J = 10.4 Hz, 1H), 5.95 (d, J = 10.4 Hz, 1H), 5.17 (s, 2H), 4.77 (dd, J = 11.2 Hz, 1.6 Hz, 1H), 2.34 (dq, J = 12.1 Hz, 6.9 Hz, 1H), 2.15 (s, 3H), 2.0−1.96 (m, 1H), 1.83−1.60 (m, 3H), 1.48 (td, J = 12.8 Hz, 4.4 Hz, 1H), 1.26 (s, 3H),1.23 (d, J = 6.9 Hz, 3H), 13C-NMR (100 MHz, CDCl3), δ, ppm: 12.0, 12.5, 20.0, 25.0, 28.0, 39.0, 40.74, 40.99, 53.41, 74.0, 82.0, 112.91, 120.0, 125.18, 128.15, 129.0, 138.8, 142.0, 145.0, 152.0, 166.0, 176.0, MS (EI,70 eV): *m:z (%):* 419 (M) [100].

https://doi.org/10.1016/j.heliyon.2019.e01366

- (*1R,2R,8aS*)-*1*-(*2-hydroxyethyl*)-*2,5,5,8a-tetramethyldecahydronaphthalen-2-ol* (FP7). A procedure described in literature was followed (Zoretic and Fang, 1998). The product was a white solid (0.3 g, 70%). Mp:(Zoretic and Fang, 1998), Molecular formula:C16 H30 O2, MW: 254,41 g/mol, 1H-NMR (400 MHz, CDCl3), δ, ppm: [92], 13C-NMR (100 MHz, CDCl3), δ, ppm (Zoretic and Fang, 1998).
- (*3aR*)-*(+)-Sclareolide Thionolactone* (FP8). A procedure described in literature was followed (Costa et al., 2005). The product was a pale yellow granular oil (0.25 g, 24%). Mp: 156 °C, Molecular Formula: C16H26OS, MW: 266,17 g/mol, 1H-NMR (400 MHz, CDCl3), δ, ppm: [95], 13C-NMR (100 MHz, CDCl3), δ, ppm: [95], MS (EI,70 eV): m/z (%) = 266.94 [M] (100).

3.2. Docking studies

Nowadays it is always more evident that water not only effects biomolecular interactions, but it is part of the interaction itself. One strategy in drug design is, therefore, to structurally modify lead molecules in order to displace water from the binding pocket of the protein upon ligand binding.

Results of the molecular modeling performed through the WATGEN algorithm are shown in Table 1. It was possible to predict the water network and its contribution to the overall affinity of the complex; it also allows a qualitative description of this network identifying molecules that form key water bridges.

Table 1. Celecoxib and sesquiterpenes calculated binding affinity and water involvement in binding to the COX-2 active site.

Compound	Binding affinity Kcal/mol	Stabilized water	Destabilized water	Displaced water
Celecoxib	−11.9	2	9	14
α-Santonin	−9.2	3	8	5
Sclareolide	−7.0	2	3	7
Leucodin	−8.8	3	11	5
FP1	−9.3	Not found	Not found	Not found
FP2	−9.3	3	8	7
FP3	−9.1	6	9	13
FP4	−8.7	3	10	11
FP5	−8.8	2	8	13
FP6	−9.4	3	9	7
FP7	−6.5	1	6	7
FP8	−6.6	1	4	9
FP9	−9.2	2	9	17

https://doi.org/10.1016/j.heliyon.2019.e01366

A tridimensional view of the comparison of the best poses is also shown in Fig. 4. Santonin and four of its derivatives (FP2, FP4, FP6 and FP9) as well as leucodin and sclareolide place the lactone towards the residues Tyr385 and Ser530. Surprisingly, FP5 and FP3 aim at the lobby of the active site with the lactone, while placing the oxime ether moiety towards Tyr385 and Ser530.

FP6, which shows the best binding affinity among the α-santonin derivatives, places the lactone towards Tyr385 and Ser530 (Fig. 5). The small water network involved here is not isolated, though; it is connected to the network surrounding the oxime moiety to form one water web. The trifluoro-methyl substituent gets close to Leu359 and Val116, but unlike in FP4, this time the less bulkiness and orientation of the moiety still let enough space for Arg 120 to interact. In fact, the latter residue is connected through several water bridges to the oxygen of the oxime along with Tyr355. The nitrogen of the oxime forms a single water bridge with Ala527.

From the predictions shown in Table 1, it seems obvious that sclareolide does not have an advantageous interaction with the binding pocket, nor do its derivatives. Actually, performing chemical modifications on the lactone moiety (FP7 and FP8) decreases the binding affinity leading also to a higher number of destabilized water molecules.

Speaking of α-santonin, this sesquiterpene shows a remarkable value of binding affinity, even though there is not a strong displacement of water molecules, such as the

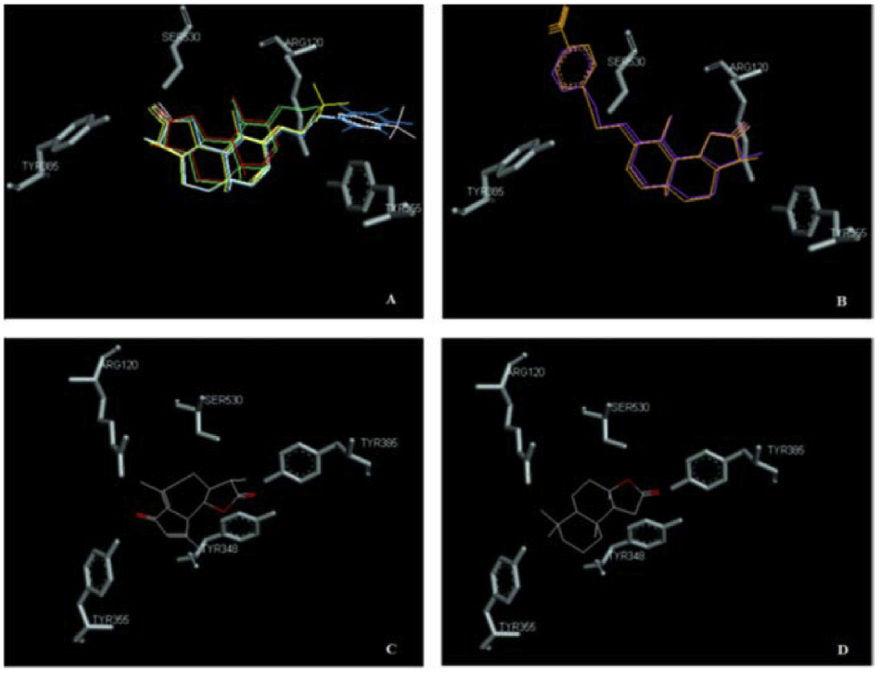

Fig. 4. Comparison of different ligands. A) α-santonin (red), FP2 (green), FP4 (blue), FP6 (yellow), FP9 (white); B) FP3 (orange), FP5 (purple); C) leucodin; D) sclareolide.

https://doi.org/10.1016/j.heliyon.2019.e01366

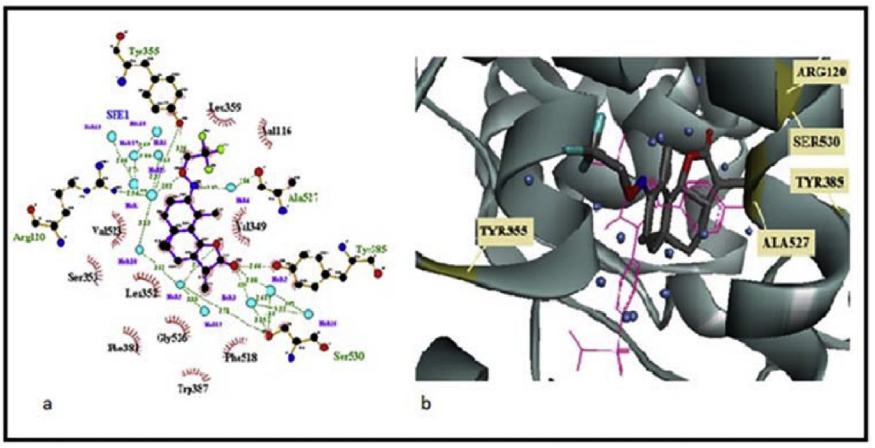

Fig. 5. (a) Ligplot 2D plot of FP6-COX2 docking; (b) FP6-COX2 docking with superimposition of Celecoxib (pink).

one seen with celecoxib. Modifications on the ketone moiety led to different behaviours.

Starting from the very simple phenyl group on FP5, it negatively affects the binding affinity and so does the similar, even bulkier, aromatic ring present in FP4. The presence of an electron-withdrawing group at the *para* position does not have any remarkable effect. Although, whether displacing a certain water molecule will help depends on a balance between the enthalpy of contacts of the water molecule and the entropy change when transferring it to the bulk solvent. Therefore, these predictions cannot be used for overall conclusions on the real affinity and/or activity of the synthesized compounds. Keeping in mind the usefulness of molecular docking for future chemical modifications, it seemed clear that biological evaluations were necessary before proceeding.

3.3. Biological evaluations

3.3.1. COX-2 inhibition

The first biological test was carried out in order to verify the real capacity of the synthesized compounds to inhibit the activity of COX-2 enzyme, *in vitro*. The results obtained, shown in Table 2, displayed that some α-santonin derivatives, FP5 and FP6, are characterized by higher inhibitory activity on the isolated enzyme compared to the parent natural compound. The compound that showed the best activity was found to be FP6, in agreement with the previous molecular docking studies. This promising result highlights the anti-inflammatory potential of this sesquiterpenic derivative, requiring further investigation to clarify its activity in more complex biological systems.

https://doi.org/10.1016/j.heliyon.2019.e01366

Table 2. COX-2 inhibition assay.

Compound	% of inhibition at 1 μM[a]
FP1	45.4
FP2	25.4
FP4	n.a.[b]
FP5	67.8
FP6	74.3
FP7	27.7
FP8	n.a.[b]
FP9	20.6
Sclareolide	58.6
Santonin	65.3

[a] n = 6, SEM ≤ 5%.
[b] n.a.: non-active.

3.3.2. Inhibition of PGE2 production in human blood

In order to better characterize the anti-inflammatory properties of FP6, the compound that showed the most promising activity in previous *in silico* and *in vitro* assays, a human whole blood assay has been used to assess its ability to produce COX-2 inhibition. In particular, an immunoenzymatic assay has been used to quantify prostaglandin E2 (PGE2) in heparinized peripheral blood aliquots, from healthy volunteers. For this purpose, the different samples were incubated with various concentrations of compound for 24 h at 37 °C, both in the absence and in the presence of 10 μg/mL LPS. PGE2 are mainly produced by COX-2 enzyme in the arachidonic acid cascade and responsible of recruitment and infiltration of immune cells. Results have shown the ability of FP6 to produce a dose-dependent reduction of PGE2 levels which reached 73% at 1 mM FP6 (Fig. 6). These results are in agreement with previous works that highlight the ability of sesquiterpenes to determine a reduction in synthesis and release of prostaglandins in human blood and other inflammation models (Zhu et al., 2013; Kim et al., 2013).

3.3.3. Effects of sesquiterpene lactones on viability and PGE2 production of LPS-stimulated RAW 264.7 cells

The effects of natural and semi-synthetic sesquiterpene lactones have been then studied in LPS-stimulated RAW 264.7 cells, a murine macrophages cellular line representing a well validated inflammation model. First of all, cells were subjected to viability assay after treatment with compounds under investigation, in order to uncover any cytotoxic effects at concentrations ranging from 12.5 to 100 μM. Santonin and its semi-synthetic derivatives did not show any cytotoxic effect, except for FP4 that has shown significant effects on cell viability from a concentration of 50 μM. On

https://doi.org/10.1016/j.heliyon.2019.e01366

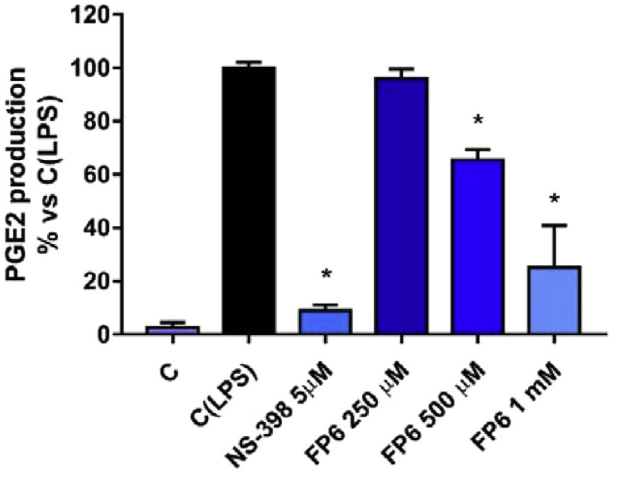

Fig. 6. Effect of FP6 on PGE2 release in human whole blood. Data are expressed as mean ± S.D. of three independent experiments, each one performed with triplicate samples. NS-398 has been used as positive control. *(P value < 0.05).

the other hand, Santonin displayed toxic effects only at 100 μM and, in addition, its derivatives FP7 and FP8 displayed a toxicity profile drastically weaker than that of their natural parent compound (Fig. 7A).

The ability of FP6 to inhibit COX-2, in this alternative inflammation model, has been investigated by quantifying PGE2 production after cell treatment. Results highlight a dose-dependent inhibition of PGE2 by FP6 at lower concentration than those used in above reported human blood assay (Fig. 7B).

3.3.4. COX-2 expression in RAW 264.7 cells

The reduction of PGE2 elicited by FP6, prompted us to hypothesize its direct inhibitory effect on COX-2. However, this result could be also due to a reduction of COX-2 expression levels, rather than its direct inhibition. In order to understand whether FP6-produced reduction of PGE2 levels is due exclusively to a direct enzyme inhibition or also to the coexistence of other molecular mechanisms, COX-2 expression has been evaluated in LPS-stimulated RAW 264.7 cells, after treatment with FP6. Surprisingly, results highlighted the ability of FP6 to produce a down-regulation of COX-2 expression (Fig. 8A). This result seems to suggest that FP6, in addition to determining inhibition of COX-2 as observed in the above-mentioned assay performed on purified enzyme, may also cause anti-inflammatory effects through different upstream mechanisms, opening new scenarios on Santonin-derivatives mode of action.

3.3.5. Nitric oxide production in RAW 264.7 cells

To better understand the molecular mechanism underlying FP6 activity, we decided to investigate its ability to modulate the functions controlled by NF-kB, the most

https://doi.org/10.1016/j.heliyon.2019.e01366

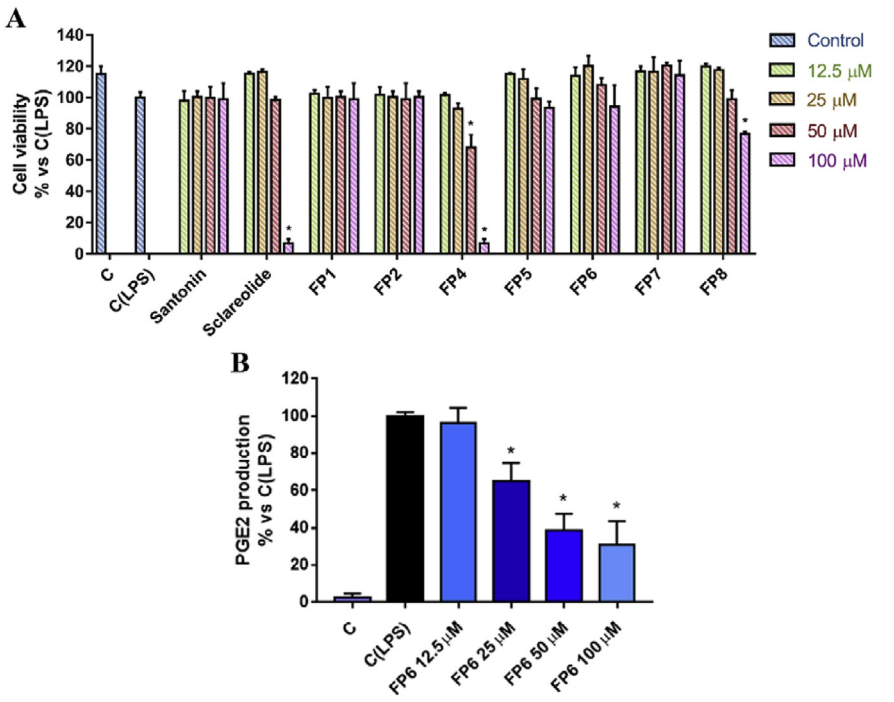

Fig. 7. (A) Cell viability assessment after treatment of LPS-stimulated RAW 264.7 cell line with different concentration (12.5−100 μM) of tested compounds for 24 hours. Results, quantified by MTT assay, are expressed as percentage of cell viability versus control (C (LPS), LPS-stimulated cells treated with DMSO). (B) Effect of FP6 on PGE2 release in LPS-stimulated RAW 264.7. NS-398 has been used as positive control. Values represent mean ± S.D. of three independent experiments, each one performed with triplicate samples. *(P value < 0.05).

important transcription factor responsible of transduction of the inflammatory signal (Tak and Firestein, 2001). One of the targets of this important transcription factor is the inducible Nitric Oxide synthase (iNOS), responsible for the synthesis of Nitric Oxide (NO), a key mediator of inflammatory pathway. For this reason, Santonin, Sclareolide and respective derivatives have been tested on LPS-stimulated RAW 264.7 cells, in order to investigate their ability to modulate NO production. Concentrations of compounds up to 100uM have been used and, as showed in Fig. 8B, Santonin was not able to decrease NO production, instead its derivatives, in particular FP5 and FP6, were characterized by interesting activity at not toxic concentrations (Fig. 8B). In the same experiment, Sclareolide evidenced a good activity, as well as its less toxic derivatives FP7 and FP8. IC_{50} values of NO production for the most active compounds have been calculated and compared to the one characterizing Diclofenac, a commonly used nonsteroidal anti-inflammatory drug (NSAID) (Table 3). These results confirm that the anti-inflammatory properties characterizing FP6 are due to mechanisms interfering with the NF-kB pathway, in agreement with previous studies on Santonin derivatives and, in general, SLs such as inhibitors of the NF-kB pathway (Tamura et al., 2012; Siedle et al., 2004).

https://doi.org/10.1016/j.heliyon.2019.e01366

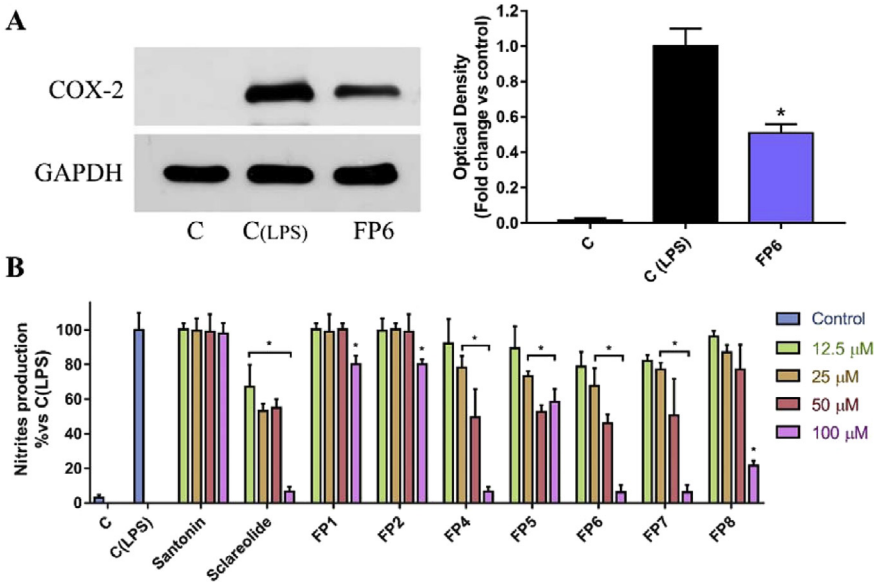

Fig. 8. (A) Effect of FP6 on COX-2 expression in LPS-stimulated RAW 264.7. C represents not stimulated RAW 264.7 cells, C (LPS) and FP6 represent LPS-stimulated cells treated with DMSO or 100μM FP6, respectively. COX-2 expression is measured as OD (Optical Density) as a ratio between the signal for COX-2 and the signal for GAPDH. (B) Nitrites production assessment after treatment of LPS-stimulated RAW 264.7 cell line with different concentration (12.5−100 μM) of tested compounds for 24 hours. Results, quantified by Griess assay, are expressed as percentage of nitrites production versus control (C (LPS), cells treated with DMSO).

Table 3. Effects of tested compound on nitrites production.

Compound	IC_{50} (μM)	95% Confidence interval
FP5	86.5	60.93 to 126.8
FP6	36.17	24.9 to 52.47
FP7	43.23	26.86 to 70.14
FP8	85.2	52.07 to 148.2
Diclofenac	134.09	84.75 to 205.37

Data are presented as IC50 values (μM) and 95% confidence intervals, obtained by nonlinear regression analysis of three independent experiments. Diclofenac has been used as a positive control.

3.3.6. Activity in RIF-1 cells, following photodynamic therapy

Photodynamic Therapy (PDT), is a form of phototherapy that involves the administration of a photosynthesizer (PS) followed by localized exposure of target tissue to the photosynthesizer's adsorbing light. PDT using Photofrin (PH), a photosynthesizer of the porphyrins group, is approved for the clinical treatment of solid tumors (Gomer et al., 1989). The therapy causes cytotoxicity of the malignant cells due to the direct effect of the PH-PDT-mediated oxidative stress, but also effects the non-malignant tumor microenvironment. This indirect action leads to

https://doi.org/10.1016/j.heliyon.2019.e01366

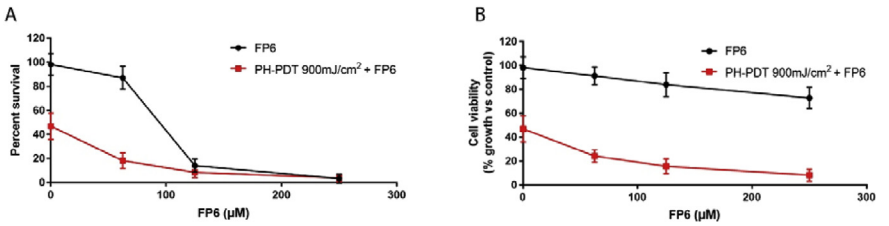

Fig. 9. (A) Cell survival: Clonogenic assay determines Percent Survival (plates were stained and colonies counted 9 days post treatment) Approximate IC50 calculated using data from clonogenic assay = 86.82 μM; (B) Cell Viability: WST1 assay determines Percent Viability at a given time point (24 hours after treatment).

inflammatory and proangiogenic responses including the induced expression of prosurvival molecules such as vascular endothelial growth factor, matrix metalloproteinases and COX-2. It seems obvious that inhibitors against inflammatory and/or angiogenic factors increase the treatment responsiveness following PDT. In fact, adjunctive administration of the COX-2 inhibitors Celecoxib and NS-398 improved PDT by increasing in vitro apoptosis and decreasing the levels of PGE-2 and vascular endothelial growth factor(Ferrario et al., 2002). For all these reasons, it was decided to evaluate the activity of santonin, sclareolide and their synthetic derivatives on mouse radiation induced fibrosarcoma cells (RIF-1), following PDT.

FP6 turned out to be the only sesquiterpene derivative able to produce in PDT treated RIF-1 cells a reduction in COX-2 expression levels and PGE_2 production at concentrations that do not affect significantly cell viability (Figs. 9, 10, 11). This result confirms again the importance of the *trifluoromethyl*-substituent in enhancing the anti-inflammatory activity of SLs.

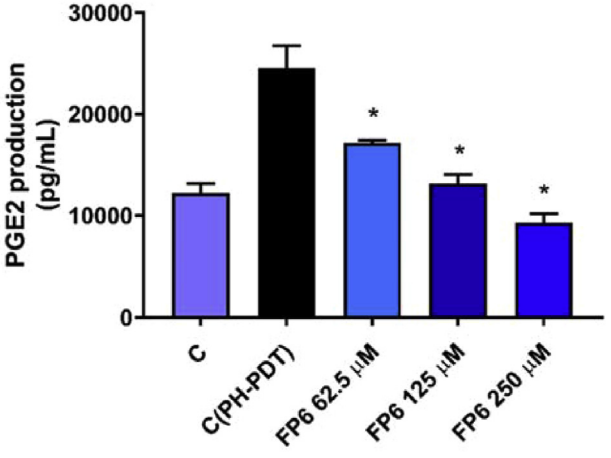

Fig. 10. Effect of FP6 on PGE2 release in PDT treated RIF-1. Values represent mean ± S.D. *(P value < 0.05).

https://doi.org/10.1016/j.heliyon.2019.e01366

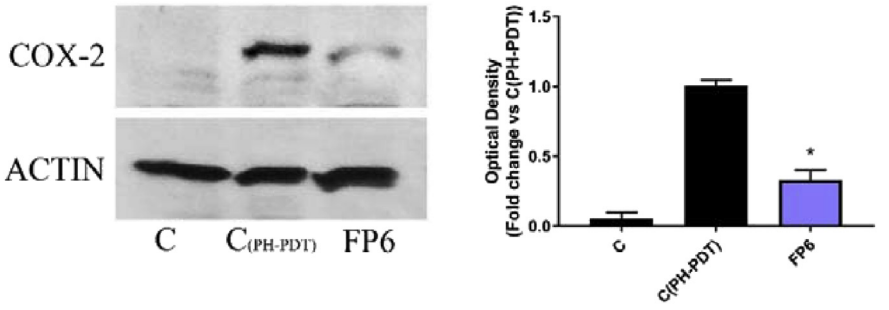

Fig. 11. Effect of FP6 on COX-2 expression in PDT treated RIF-1. C represents not stimulated RIF-1 cells, C(PH-PDT) and FP6 represent treated cells with PDT and Ethanol or PDT and 250μM FP6, respectively. COX-2 expression is measured as OD (Optical Density) as a ratio between the signal for COX-2 and the signal for actin.

4. Conclusions

All tested molecules fit well in the binding pocket, although a remarkable reduction both in the expression and the activity of the enzyme, as well as in the concentration of PGE2 is noticeable just at high concentrations. The only noteworthy compound is FP6, which positive results in terms of biological activity agree with predictions made through molecular modeling. Its CF3 moiety is very well-known in pharmaceutical chemistry due to its flexibility and peculiar chemical and physiological stability (Yale, 1958). It is also present in celecoxib itself. Therefore, it seems right to proceed on this path for future derivatives and studies.

Declarations

Author contribution statement

Luca Frattaruolo: Conceived and designed the experiments; Performed the experiments; Analyzed and interpreted the data; Wrote the paper.

Filomena Perri: Conceived and designed the experiments; Wrote the paper.

Matteo Brindisi: Conceived and designed the experiments; Performed the experiments.

Ian Haworth: Conceived and designed the experiments.

Angela Ferrario: Performed the experiments; Analyzed and interpreted the data.

Asma El-magboub, Charles Gomer: Performed the experiments.

James Adams: Contributed reagents, materials, analysis tools or data.

Francesca Aiello: Contributed reagents, materials, analysis tools or data; Wrote the paper.

https://doi.org/10.1016/j.heliyon.2019.e01366

Funding statement

This research did not receive any specific grant from funding agencies in the public, commercial, or not-for-profit sectors.

Competing interest statement

The authors declare no conflict of interest.

Additional information

No additional information is available for this paper.

Acknowledgements

We thank Professor Anna Rita Cappello for her generous help in the planning of experiments performed on RAW 264.7 cell line and on human blood, as well as in writing the manuscript.

References

Abid, M., Husain, K., Azam, A., 2005. Synthesis and antiamoebic activity of new oxime ether derivatives containing 2-acetylpyridine/2-acetylfuran. Bioorg. Med. Chem. Lett. 15, 4375−4379.

Adams, J., 2012. The use of California sagebrush (*Artemisia californica*) liniment to control pain. Pharmaceuticals 5, 1045−1053.

Al-Harbi, M.M., Qureshi, S., Ahmed, M.M., Raza, M., Miana, G., Shah, A.H., 1994. Studies on the antiinflammatory, antipyretic and analgesic activities of santonin. Jpn. J. Pharmacol. 64, 135−139.

Allaby, M., 2006. A Dictionary of Plant Sciences. Oxford University Press.

Arantes, F., Barbosa, L., Maltha, A., Demuner, P., Marcal da Costa, J., Ferreira, L., Pessoa, ., 2010. Synthesis of novel α-santonin derivatives as potential cytotoxic agents. Eur. J. Med. Chem. 45 (12), 6045−6051.

Bonesi, M., et al., 2018. Exploring the anti-proliferative, pro-apoptotic, and antioxidant properties of Santolina corsica Jord. & Fourr. (Asteraceae). Biomed. Pharmacother. 107, 967−978.

Bui, H., Schiewe, A., Haworth, I., 2007. WATGEN: an algorithm for modeling water networks at protein−protein interfaces. J. Comput. Chem. 28, 2241−2251.

https://doi.org/10.1016/j.heliyon.2019.e01366

Carullo, G., Galligano, F., Aiello, F., 2017. Structure−activity relationships for the synthesis of selective cyclooxygenase 2 inhibitors: an overview (2009−2016). Med. Chem. Commun. 8, 492−500.

Chen, H., et al., 2014. Synthesis and structure-activity relationships of guaiane-type sesquiterpene lactone derivatives with respect to inhibiting NO production in lipopolysaccharide-induced RAW 264.7 macrophages. Eur. J. Med. Chem. 83, 307−316.

Coricello, A., El-Magboub, A., Luna, M., Ferrario, A., Ian S. Haworth, I.S., Charles J. Gomer, J.C., Aiello, F., Adams, J.D., 1 April 2018. Rational drug design and synthesis of new α-Santonin derivatives as potential COX-2 inhibitors. Bioorg. Med. Chem. Lett. 28 (6), 993−996.

Costa, M. d., Teixeira, S.G., Rodrigues, C.B., Figueiredo, P.R., Curto, M.J., 2005. A new synthesis of (−)-thioambrox and its 8-epimer. Tetrahedron 61, 4403−4407.

Di Gioia, M.L., Leggio, A., Malagrinò, F., Romio, E., Siciliano, C., Liguori, A., 2016. N-methylated α-amino acids and peptides: synthesis and biological activity. Mini Rev. Med. Chem. 16 (9), 683−690.

Ferrario, A., Tiehl, K. v., Wong, S., Luna, M., Gomer, C.J., 2002. Cyclooxygenase-2 inhibitor treatment enhances photodynamic therapy-mediated tumor response. Cancer Res. 62, 3956−3961.

Fontaine, P., Wong, V., Williams, T., Garcia, C., Adams, D., 2013. Chemical composition and antinociceptive activity of California sagebrush (*Artemisia californica*). J. Pharmacogn. Phytother. 5 (1), 1−11.

Frattaruolo, L., Lacret, R., Cappello, A.R., Truman, A.W., 2017. A genomics-based approach identifies a thioviridamide-like compound with selective anticancer activity. ACS Chem. Biol. 11 (12), 2815−2822.

Gerke, T., Satler, A., & Mullner, S. (2001). Anti-inflammatory active ingredients. Patent PCT/EP01/11055.

Ghantous, A., Gali-Muhtasib, H., Vuorela, H., Saliba, N., Darwiche, N., 2010. What made sesquiterpene lactones reach cancer clinical trials? Drug Discov. Today 15, 668−678.

Giordano, O., Guerreiro, E., Pestchanker, M., Guzman, J., Pastor, D., Guardia, T., 1990. The gastric cytoprotective effect of several sesquiterpene lactones. J. Nat. Prod. 53, 803−809.

Gomer, C.J., Rucker, N., Ferrario, A., Wong, S., 1989. Properties and applications of photodynamic therapy. Radiat. Res. 120 (1), 1−18.

 https://doi.org/10.1016/j.heliyon.2019.e01366

Good, R., 1974. The Geography of the Flowering Plants, fourth ed. Longman, London.

Hayet, E., Fatma, B., Souhir, I., Waheb, F., Abderaouf, K., Mahjoub, A., Maha, M., 2007. Antibacterial and cytotoxic activity of the acetone extract of the flowers of Salvia sclarea and some natural products. Pak. J. Pharm. Sci. 20 (2), 146−148.

Huang, G., Pan, C., Wu, C., 2012. Sclareol exhibits anti-inflammatory activity in both lipopolysaccharide-stimulated macrophages and the λ-carrageenan-induced paw edema model. J. Nat. Prod. 75 (1), 54−59.

Kang, T., Kim, Y., Lee, D., Wang, Z., Chang, S., 2014. Iridium-catalyzed intermolecular amidation of sp3 C−H bonds: late-stage functionalization of an unactivated methyl group. J. Am. Chem. Soc. 136 (11), 4141−4144.

Kim, H., Yang, J., Han, E., Choi, J., Khanal, T., Jeong, M., Jeong, H., 2013. Inhibitory effect of dihydroartemisinin against phorbol ester-induced cyclooxygenase-2 expression in macrophages. Food Chem. Toxicol. 56, 93−99.

Klayman, D.L., 1993. Artemisia annua: from weed to respectable antimalarian plant. In: Kinghorn, A.B. (Ed.), Human Medicinal Agents from Plants, vol. 534. ACS Symp. Series, Washington DC, pp. 242−255. ISSN: 0097-6156.

Lee, H., Lara, P., Ostuni, A., Presto, J., Johansson, J., Nilsson, I., Kim, H., 2014. Live-cell topology assessment of URG7, MRP6$_{102}$ and SP-C using glycosylatable green fluorescent protein in mammalian cells. Biochem. Biophys. Res. Commun. 450 (4), 1587−1592.

Li, Y., Sutch, B., Bui, H., Gallaher, T., Haworth, I.S., 2011. Modeling of the water network at protein-RNA interfaces. J. Chem. Inf. Model. 51, 1347−1352.

Merkhatuly, N., Zhokizhanova, S., Balmagambetova, L., Adenekov, S., 2007. Oximation of α-santonin. Russ. J. Org. Chem. 43 (1), 150−151.

Messaudene, D., 2011. Ex vivo effects of flavonoids extracted from *Artemisia herba-alba* on cytokines and nitric oxide production in Algerian patients with Adamantiades-Behcet's disease. J. Inflamm. 8, 35.

Platts, J.A., Howard, S.T., Bracke, a. B., 1996. Directionality of hydrogen bonds to sulfur and oxygen. J. Am. Chem. Soc. 118 (11), 2726−2733.

Rodriguez, E., Towers, G., Mitchell, J., 1976. Biological activities of sesquiterpene lactones. Phytochemistry 15, 1573−1580.

Schmidt, B., Belolipov, I., Kurmukov, A., Zakirov, S., & I., R. (2008). Sesquiterpene lactone extract from Artemisia leucodes for reducing inflammation and down regulating pro-inflammatory gene expression . US Patent US2008/0145465 A1.

https://doi.org/10.1016/j.heliyon.2019.e01366

Schwarz, O., et al., 2007. Natural products in parallel chemistry–novel 5-lipoxygenase inhibitors from BIOS-based libraries starting from alpha-santonin. J. Comb. Chem. 9 (6), 1104−1113.

Siedle, B., Garcia-Pineres, A., Murillo, R., Schulte-Monting, J., Castro, V., Rungeler, P., Merfort, I., 2004. Quantitative structure-activity relationship of sesquiterpene lactones as inhibitors of the transcription factor NF-KB. J. Med. Chem. 47, 6042−6054.

Simonsen, H.T., Weitzel, C., Christensen, S.B., 2013. Guaianolide sesquiterpenoids:pharmacology and biosynthesis. In: Natural Products. Springer-Verlag, pp. 3069−3098.

Siracusa, L., Saija, A., Cristani, M., Cimino, F., D'Arrigo, M., Trombetta, D., Ruberto, G., 2011. Phytocomplexes from liquorice (Glycyrrhiza glabra L.) leaves − chemical characterization and evaluation of their antioxidant, anti-genotoxic and anti-inflammatory activity. Fitoterapia 82 (4), 546−556.

Soltani Rad, M.N., Khalafi-Nezhad, A., Karimitabar, F., Behrouz, S., 2010. An efficient one-pot synthesisof oxime ethers from alcohols using triphenylphosphine/carbon tetrachloride. Synthesis 2010 (10), 1724−1730.

Tak, P.P., Firestein, G.S., 2001. NF-kappaB: a key role in inflammatory diseases. J. Clin. Invest. 1 (107), 7−11.

Tamura, R., et al., 2012. Santonin-related compound 2 inhibits the nuclear translocation of NF-κB subunit p65 by targeting cysteine 38 in TNF-α-induced NF-κB signaling pathway. Biosci. Biotechnol. Biochem. 76 (12), 2360−2363.

Timbrook, J., 1990. Ethnobotany of Chumash Indians, California, based on collections by John P. Harrington. Econ. Bot. 44 (2), 236−253.

Tundis, R., Frattaruolo, L., Carullo, G., Armentano, B., Badolato, M., Loizzo, M., Cappello, A., 2018. An ancient remedial repurposing: synthesis of new pinocembrin fatty acid acyl derivatives as potential antimicrobial/anti-inflammatory agents. Nat. Prod. Res. 20, 1−7.

White, E.H., Eguchi, S., Marx, J.N., 1969. The synthesis and stereochemistry of desacetoxymatricarin and stereochemistry of matricarin. Tetrahedron 25, 2099−2115.

Wierzejewska, M., Sałdyka, M., 2004. Are hydrogen bonds to sulfur and oxygen different? Theoretical study of dimethylsulfide and dimethylether complexes with nitric acid. Chem. Phys. Lett. 391, 143−147.

Willcox, M., 2009. Artemisia species: from traditional medicines to modern antimalarians and back again. J. Altern. Complement. Med. 15 (2), 101−109.

https://doi.org/10.1016/j.heliyon.2019.e01366

Wright, C.W., 2002. Artemisia. Taylor and Francis, London.

Yale, H.L., 1958. The trifluoromethyl group in medical chemistry. J. Med. Pharm. Chem. 1 (2), 121–133.

Zhong, Y., Huang, Y., Santoso, M.B., Wu, L.D., 2012. Sclareol exerts anti-osteoarthritic activities in interleukin-1β-induced rabbit chondrocytes and a rabbit osteoarthritis model. Int. J. Clin. Exp. Pathol. 8 (3), 2365–2374. PMID: 26045743.

Zhu, X., Yang, L., Li, Y., Zhang, D., Chen, Y., Kostecká, P., Zídek, Z., 2013. Effects of sesquiterpene, flavonoid and coumarin types of compounds from Artemisia annua L. on production of mediators of angiogenesis. Pharmacol. Rep. 65 (2), 410–420.

Zoretic, P.A., Fang, H., 1998. Synthesis of acuminolide and 17-O-acetylacuminolide from (+)-sclareolide. J. Org. Chem. 63 (4), 1156–1161.

https://doi.org/10.1016/j.heliyon.2019.e01366